



## CFD Letters

Journal homepage:

[https://semarakilmu.com.my/journals/index.php/CFD\\_Letters/index](https://semarakilmu.com.my/journals/index.php/CFD_Letters/index)

ISSN: 2180-1363



## Performance Optimization of a Simulation Study on Phase Change Material for Photovoltaic Thermal

Mohd Afzanizam Mohd Rosli<sup>1,2</sup>, Siti Nur Dini Noordin Saleem<sup>1,\*</sup>, Nortazi Sanusi<sup>1</sup>, Nurfarhana Salimen<sup>1</sup>, Safarudin Gazali Herawan<sup>3</sup>, Qaharuddin Abdullah<sup>4</sup>

<sup>1</sup> Fakulti Kejuruteraan Mekanikal, Universiti Teknikal Malaysia Melaka, Hang Tuah Jaya, 76100 Durian Tunggal, Melaka, Malaysia

<sup>2</sup> Centre for Advanced Research on Energy, Universiti Teknikal Malaysia Melaka, Hang Tuah Jaya, 76100 Durian Tunggal, Melaka, Malaysia

<sup>3</sup> Industrial Engineering Department, Faculty of Engineering, Bina Nusantara University, Jakarta, 11430 Indonesia

<sup>4</sup> Malaysian Industry-Government Group for High Technology, MIGHT Partnership Hub, Jalan IMPACT, 63000 Cyberjaya, Selangor, Malaysia

### ARTICLE INFO

#### Article history:

Received 11 May 2022

Received in revised form 23 June 2022

Accepted 15 July 2022

Available online 30 September 2022

#### Keywords:

Photovoltaic Thermal; Phase Change Material; Computational Fluid Dynamics (CFD); Efficiency; Paraffin Wax

### ABSTRACT

The integration of Phase Change Material (PCM) with the Solar Photovoltaic Thermal (PVT) serves as heat storage to enhance the system's performance. Temperature rises have an undesirable effect on efficiency results in a diminishment in the amount of energy produced by the solar panel. Parametric analysis and temperature investigation are involved in improving the performance of the system. The variation of performance will assist in developing an optimized PVT-PCM system. The model is validated by comparison from published journals on the studies related to phase change material implemented in solar PVT. For the variation of mass flow rate, the overall efficiencies achieved by 10 kg/h, 30 kg/h, 50 kg/h and 70 kg/h are 90.82%, 90.54%, 90.48% and 90.46%, respectively. In addition, solar irradiance of 200 W/m<sup>2</sup>, 450 W/m<sup>2</sup> and 800 W/m<sup>2</sup> produced 91.17%, 90.82% and 90.33% of overall efficiencies. Increased in flow rate requires stronger pumps which increase the total cost of the system. Therefore, identifying the optimal flow rate might help to achieve an appropriate thermal efficiency while sustaining in low costs. Finally, this paper presented a numerical investigation of PCM acts as promising elements incorporated in the PVT system that has the capability to reduce the temperature of the PVT-PCM system.

## 1. Introduction

International energy demand is rising rapidly, leading opportunities to examine into the availability of alternative energy sources as a solution. Energy from non-renewable resources such as natural gas, fossil fuels, petroleum, coal, or nuclear sources is referred to as conventional energy. Renewable energy, on the other hand, is a type of energy that is derived from naturally renewing and never diminishing energy resources. By 2050, renewable energy is expected to account for roughly 67% of the world's energy consumption. The road plan predicts that by the year 2020, renewable energy sources will account for 58% of electric power generation, 29% of heating, and 13% of transportation [1].

\* Corresponding author.

E-mail address: [sitinurdini.noordin@gmail.com](mailto:sitinurdini.noordin@gmail.com) (Siti Nur Dini Noordin Saleem)

<https://doi.org/10.37934/cfdl.14.9.3251>

Solar energy is accomplished using a range of devices that use a variety of light energy conversion techniques to be able to produce useful energy harvesting from solar energy conversion [2]. The conversion system in solar are absolutely critical for solar energy's powerful commercialisation. Numerous conversion processes are used to transform solar energy into usable energy such as photoelectric (solar photovoltaic system), photoelectric-thermal (solar photovoltaic thermal system), and photothermal (solar collectors) [3]. The performance of these systems is mostly determined by the properties of the working fluid and cooling medium used in energy conversion or conveyance [4,5].

In research from Abdul-Ganiyu *et al.*, [6] the development in solar technologies introduces progressive development throughout the years. Integration between the conventional PV system into thermal system helps in the efficiencies and increases the performance of the PVT system. Since the operations will not be focused on one process making solar PVT, the performance of solar PVT produces higher than solar PV system. Solar PVT system able to heat the output water as solar heaters and generate energy from the solar modules. The advancements in solar thermal technology, particularly the PVT system have been introduced comprehensively by Fu *et al.*, [7]. The present PVT system is primarily composed of two types: PVT air collector systems and PVT water collector systems. In addition, Phase change materials (PCM) are compounds that possess the ability in thermal energy storage which allowing for temperature stability. Hence, in this research reviews the evidence for the development of Solar PVT integrated with Phase Change Material (PCM).

Throughout decades, numerous developments have been made in solar PVT to improve their output production and efficiencies. In this research, Phase Change Material (PCM) is chosen as the passive cooling medium to increase the performance of the solar PVT. PCM has a high energy density, a nearly constant temperature, and absorb and release thermal energy throughout the melting and freezing process. As a result, PCM is well suited for solar cell heat collection. There are 3 categories of PCM in solar PVT application include organic (paraffins, fatty acids and polyethylene glycol (PEG)), inorganic (salt hydrates) and composite materials (combination of organic and inorganic) [8].

Studies of Thakur *et al.*, [9] show the PCM releases and absorbs sufficiently as a result of the phase transition. The phase transition occurs when a solid change to a liquid and vice versa, resulting in the generation of usable heat. It is possible to use PCM to store surplus thermal energy generated during peak hours and release this stored energy when the energy is required in the future.

Analyses correlation by Badieli *et al.*, [10] and Lin *et al.*, [11] the performance of a fins-incorporated PCM-based Flat Plate Collector (FPC) was examined using a CFD model and experimental simultaneously. During the study, distinct PCM materials with differing melting temperatures are utilized. The results indicate that the FPC with PCM and fin produces cooler output temperatures in the morning. The effects of the research by Thakur *et al.*, [9] on Solar PVT performance are similar to those of by Lin *et al.*, [11].

Several examples of Phase Change Material (PCM) are paraffin wax, lauric acid, sodium sulfate, benzoic acid, bees wax and glycolic acid. Preet *et al.*, [12] conducted three different systems were used: a convectional photovoltaic (PV) system, a photovoltaic thermal (PVT) system, and a photovoltaic thermal system with phase change material (PVT-PCM). PVT and PVT-PCM have a lower temperature than convectional PV panels, with a maximum temperature reduction of 47% for PVT and 53% for PVT-PCM at a mass flow rate of 0.031 kg/s of water. This view is supported by Khan *et al.*, [13] investigated the effectiveness of solar PVT by using paraffin wax and nanoparticles into the design. They determined that increasing the surface area between the PCM and the absorber plate increases to study the output temperatures. Improved results may be achieved with PCM compared to standard absorber plate with the help of new technological developments in combination of PCM with solar PVT. Recent study by Abdullah *et al.*, [14] have improved on the combination of paraffin

wax and nanoparticles. Total daily production ranges between 2500 and 5550 mL/m<sup>2</sup> when PCM is combined with CuO nanoparticles. As a result, production increased by 122%. Therefore, PCMs have been recognised for usage in the given application for a various of purposes, including rapid cooling, low thermal conductivity, phase separation, and reasonable cost.

Studies on the efficiencies of PCM integration in solar PVT shown in Table 1. Several researchers include nanofluid in their studies but nanofluid is costly. The combination with PCM such as paraffin wax leads to unreasonable price of solar PVT. In this study, nanofluid is neglected to improve the cost of the solar PVT. Most of the researchers use paraffin wax but with different thermophysical properties. From Table 1, Mousavi *et al.*, [15] shows highest overall efficiencies from various PCM (Paraffin C15, C18 and C22) with 94%, 94.7% and 95.9% respectively. On the other hand, Wahab *et al.*, [16] and Hassan *et al.*, [17], shows the lowest overall efficiency among the other researchers. Both of the researchers use the same type of paraffin wax which is RT-35HC, but the results turned out to be different due to the experimental setup and presents of nanofluid. Even though Wahab *et al.*, [16] and Hassan *et al.*, [17] used distilled water-graphene and Sodium Dodecyl Benzene Sulphonate (SDBS)-Graphene as active cooling medium respectively, the results of the overall efficiencies show between 14.80% to 31.2%. Overall, thermal efficiency, electrical efficiency and overall efficiency from other researchers are exhibited in Table 1.

A significant aspect in the performance of solar PVT is temperature changes. When the PVT temperature rises, the output current climbs exponentially while the voltage output decreases linearly. As a consequence, this may significantly reduce solar panel power production. In addition, temperature rises have an undesirable effect on the efficiency of solar panels. When the efficiency of a solar panel decreases, the solar panel energy production reduces. Hence, temperature is an important aspect that needs to be analysed to monitor the performance of the PVT. Consequently, the performance of PVT integrated with PCM are evaluated utilizing parametric analysis.

**Table 1**  
 Efficiencies of PCM used recently for PVT systems

Author	Nature of Study	Phase Change Material	Thermal Efficiency	Electrical Efficiency	Overall Efficiency
Fu <i>et al.</i> , [7]	Experiment	Microencapsulated Phase Change Material (MPCM)	58.3%	12.21%	70.51%
Abdullah <i>et al.</i> , [14]	Experiment	Paraffin wax	34%	-	34%
Mousavi <i>et al.</i> , [15]	Simulation	Paraffin C15 Paraffin C18 Paraffin C22	Paraffin C15: 81.8% Paraffin C18: 81.7% Paraffin C22: 83.5%	Paraffin C15: 12.2% Paraffin C18: 13% Paraffin C22: 12.4%	Paraffin C15: 94% Paraffin C18: 94.7% Paraffin C22: 95.9%
Wahab <i>et al.</i> , [16]	Experiment	Paraffin wax (RT-35HC)	1.78%	13.02%	14.80%
Hassan <i>et al.</i> , [17]	Experiment	Paraffin wax (RT-35HC)	20.8%	10.4%	31.2%
Shalaby <i>et al.</i> , [18]	Experiment	Paraffin wax and steric acid	35%	-	-
Al-Musawi <i>et al.</i> , [19]	Simulation	Paraffin wax	55%	14.2%	69.2%
Al-Waeli <i>et al.</i> , [20]	Experiment	Paraffin Wax	72%	13.7%	85.7%
Kazemian <i>et al.</i> , [21]	Simulation	PCM (not mentioned the type)	58%	14%	72%

Naghdbishi <i>et al.</i> , [22]	Experiment	Water/glycol-based and Organic paraffin wax	23.58%	4.21%	27.79%
Salari <i>et al.</i> , [23]	Simulation	PCM (type not mentioned)	MgO-water: 46.176% MWCNT-water: 47.168% MgO – MWCNT: 46.759%	MgO-water: 13.892% MWCNT-water: 13.912% MgO – MWCNT: 13.902%	MgO-water: 60.068% MWCNT-water: 61.080% MgO – MWCNT: 60.661%
Sopian <i>et al.</i> , [24]	Experiment	Paraffin Wax	72%	13.7%	85.7%
Carmona <i>et al.</i> , [25]	Experiment	Organic Paraffin wax (RT-35)	17.22%	14.14%	31.35%

## 2. Methodology

### 2.1 Overview of Solar PVT-PCM Model

This research presents proposed solar photovoltaic thermal integrated with phase change material (PVT-PCM). The proposed 3-dimensional model of PVT-PCM is developed using AutoCAD software to illustrate the components in simulation process. The components of PVT-PCM consists of 2 ethylene vinyl acetate (EVA), photovoltaic (PV) panel, tedlar polyvinyl fluoride (Tedlar), copper absorber plate, copper tube collector and phase change material (PCM). The copper absorber plate is positioned above PCM layer and the copper tube collector is partially immersed in the PCM layer. Subsequently, the model of the proposed PVT-PCM is represented as in Figure 1.

The chosen working fluid in this research is water. The flow of the fluid is anticipated in a uniform, laminar, fully developed and incompressible flow regime with no turbulence. A parallel array of tubes constitutes the real collector, however for the purposes of 3D simulations, only one tube collector is considered in order to decrease the computational cost [26,27]. Anti-reflection coatings (ARC) have a thickness of 0.0001 mm, which is neglected in the simulation [28]. Figure 2 illustrates the cross section implemented in the simulation process.

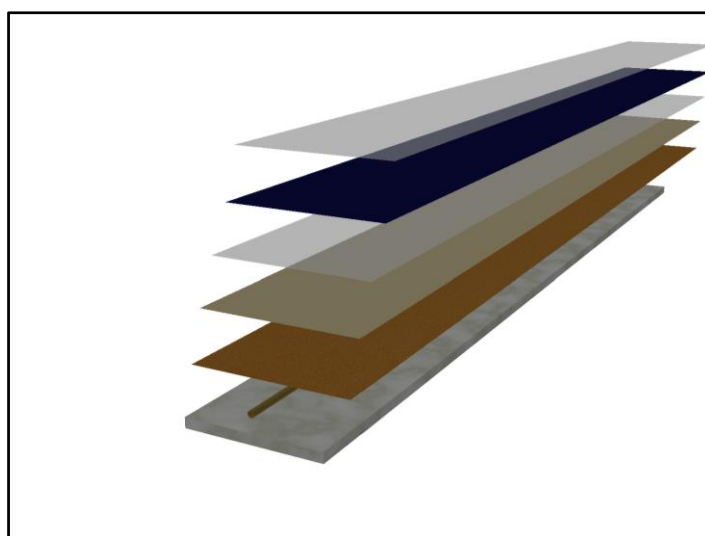


**Fig. 1.** Overview of solar PVT-PCM in 3D model

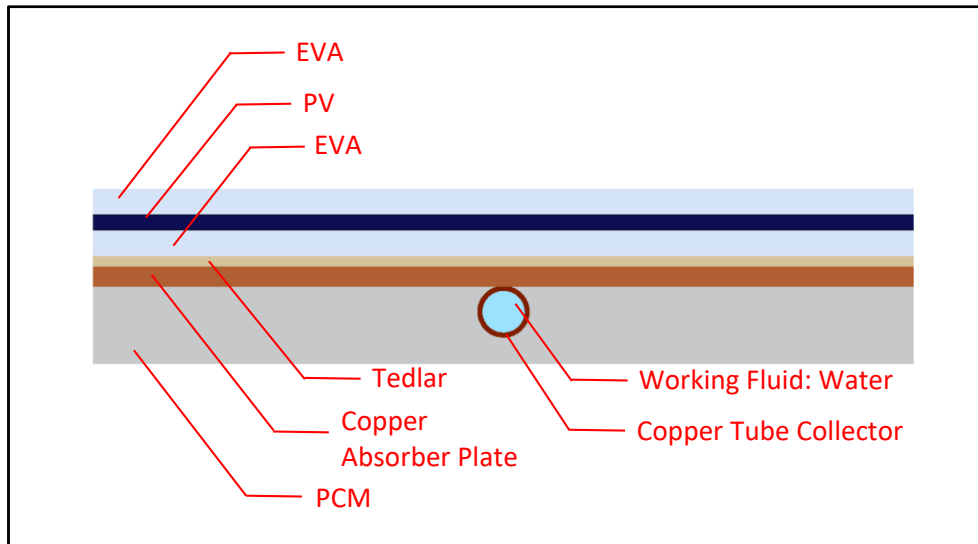


Fig. 2. Cross section of PVT-PCM model

## 2.2 Study Area

The simulation works is conducted under Malaysia climate condition at coordinate 2.3138° N and 102.3211° E. According to Malaysian Meteorological Department [29] the average monthly temperature in the lowland areas ranges from 25.9°C to 29.0°C. The average monthly sunshine hours range between 150hours and 210hours. In addition, the average number of rainy days per month varies throughout the year, ranging from 14 days (lowest) to 20 days (peak). The lowest days usually in July while the peak seasons in October, November, and April. However, the other months are moderately in between the days.

In Malaysia, the average direct solar irradiance in a year which is quite substantial for residential and industrial. According to Shavalipour *et al.*, [30] solar irradiance received by major part in Peninsular Malaysia recorded an average of approximately 450 W/m<sup>2</sup> except for the east coast in the rainy season. Furthermore, Hossain *et al.*, [31] critically examined that the maximum output from a PVT or PVT-PCM panel under average Malaysian weather conditions is approximately 1000 W/m<sup>2</sup>.

## 2.3 Fluid Flow Characteristics and Simulation Assumptions

In this proposed PVT-PCM, water is chosen as the working fluid acts as laminar fluid flow. Since the flow is laminar, the Reynolds number shows lower than 2300. The flow of the fluid is anticipated in a uniform, laminar, fully developed and incompressible flow regime with no turbulence [21]. In addition, the simulation undergoes transient flow analysis. The following assumptions are also imposed with the purpose of reducing the numerical simulation's complexity:

- i. Thermophysical properties of solid parts (PV, EVA, Tedlar, Copper Absorber Plate, Copper Tube Collector) are considered constant and do not change with temperature [21].
- ii. The contact resistance between each component in the PVT-PCM is neglected [27].
- iii. Thermophysical of PCM such as enthalpy of fusion, melting point, specific heat capacity and thermal conductivity are considered constant [32].
- iv. PV panel are considered clean without any debris [12].
- v. Solar irradiance is considered to be uniform and creates incidently in the upmost surface of the PVT-PCM which is EVA layer [15,21].

- vi. PCM is considered to have a 3-dimensional liquid phase that is incompressible, unsteady flow, and Newtonian [33].
- vii. It is considered that the EVA layer is completely transmissive [31,34].

#### 2.4 Thermophysical Properties of Phase Change Material (PCM)

Phase Change Material (PCM) manufactured by Rubitherm Technologies GmbH, Berlin, Germany (Model No: RT44HC) were employed in this simulation investigation. RT represents Rubitherm from the company’s name while HC represent a greater latent heat capacity by 25–30% and melts over a narrower temperature range as compared to traditional RT PCM.

In the melting process, the heat transmission from the PV layer passed down to the PCM layer occurs by conduction and natural convection. In the presence of solar irradiance, solid PCM begins to melt as a result of the heat gained from the thermal collector. However, when there is low presence of solar irradiance, the thermal collector will not be able to harvest solar energy. Therefore, the heat collected from the PCM previously will generate the energy for the PVT system. The PCM will start losses its heat and becomes solidified again slowly. Table 2 represents the thermophysical properties of RT44HC.

**Table 2**  
 Thermophysical Properties of RT44HC

Parameters	Symbol	RT-44 HC
Density at 25°C (kg/m <sup>3</sup> )	$\rho$	800
Melting Point (°C)	$T_{MP}$	43
Specific Heat Capacity (J/kg.K)	$C$	2000
Thermal Conductivity (W/m.K)	$\lambda$	0.2
Enthalpy of Fusion (kJ/kg)	$H$	250
Solidus Temperature (°C)	$T_{solid}$	25
Liquidus Temperature (°C)	$T_{liquid}$	80
Volume Expansion (%)	$V$	12.5

#### 2.5 Model Geometry and Components

In this study, the geometry is a development of the 3-dimensional model of solar photovoltaic thermal (PVT) integrated with phase change material (PCM) using Design Modeler or Space Claim. In this research, the interface of the Ansys geometry part is chosen Design Modeler. Material of fluid or solid was assigned at this stage. The dimension of the PVT-PCM implemented from the real size of model to reduce errors. The geometry consists of 8 parts and 8 bodies. PCM and Water are the elements assigned as fluid while other components are assigned as solid. Table 3 highlights the dimension of the components in Solar PVT-PCM system.

**Table 3**  
 Dimensions of the components of the solar PVT-PCM

Components	Dimensions (mm)		
	L	W	H
Ethylene Vinyl Acetate (EVA)	1640	200	0.5
Photovoltaic Panel (PV)	1640	200	0.3
Tedlar	1640	200	0.1
Copper Absorber Plate	1640	200	0.4
Phase Change Material (PCM)	1640	200	15
Copper Tube Collector	10 (diameter)		

Table 4 shows the thermophysical properties in each component. Tedlar polyvinyl fluoride (Tedlar) is a strong, flexible and fatigue-resistant layer while Ethylene Vinyl Acetate (EVA) is copolymer of ethylene and vinyl acetate monomers that acts a sealing layer for PVT. Subsequently, thermophysical properties of PCM as shown previously in Table 2. In Ansys Fluent setup, the thermophysical properties are fulfilled in material section.

**Table 4**  
Thermophysical Properties of the components in PVT-PCM

Components	Density (kg/m <sup>3</sup> )	Specific Heat Capacity (J/kg.K)	Thermal Conductivity (W/m.K)
Ethylene Vinyl Acetate (EVA)	960	2090	0.35
Photovoltaic Panel	2330	700	148
Tedlar	1200	1250	0.2
Copper Absorber Plate	8960	385	401
Copper Tube Collector	8960	385	401
Water	998.2	4182	0.6

Operating condition provides in Table 5 are considered as boundary condition in Ansys Fluent setup.

**Table 5**  
Operating Condition

Parameters	Value
Inlet temperature of coolant flow (°C)	30
Ambient Temperature (°C)	30
Wind Speed (m/s)	1
Solar Irradiance (W/m <sup>2</sup> )	450
Mass flow rate of coolant flow (kg/h)	10

## 2.6 Governing Equation

Beforehand proceeding with the setup setting, there are 2 types of solvers involved in Ansys Fluent. There are Pressure-Based and Density-Based. Density-Based Coupled Solver solves for continuity, momentum and energy equations. An equation of state is used to construct Pressure-Based Solver.

On the other hand, the pressure-based solvers take momentum and pressure (or pressure correction) as the primary variables. Pressure-velocity coupling algorithms are derived by reformatting the continuity equation. The pressure-based solver is applicable for a wide range of flow regimes from low speed incompressible flow to high-speed compressible flow.

### 2.6.1 Working fluid

The following equations express the mass and momentum conservation laws for the fluid domain:

$$\frac{\delta \rho_f}{\delta t} + \nabla \cdot (\rho_f \vec{V}_f) = 0 \quad (1)$$

$$\rho_f \left[ \frac{\delta \vec{V}_f}{\delta t} + (\vec{V}_f \cdot \nabla) \vec{V}_f \right] = -\nabla P + \nabla \cdot (\mu_f \nabla \vec{V}_f) \quad (2)$$

where  $\vec{V}$ ,  $P$  and  $\mu$  are fluid velocity, pressure and viscosity and subscript f represents working fluid. Heat transmission occurs by a combination of conduction and convection heat transfer in the collector's fluid field. Ansys Fluent solves in the form of the energy equation from Ansys Fluent model selection. As a result, the following is the energy equation:

$$\rho C_p \frac{\delta T_f}{\delta t} + \rho_f C_{pf} \vec{V}_f \cdot \nabla T_f = \nabla \cdot (k_f \nabla T_f) \quad (3)$$

### 2.6.2 Solid components

Due to the fact that conduction is the only mode of heat transport in the solid components of the system (i.e., the PV layers, absorber plate, and collector). The subscript s represents solid components. The following energy equation is used to describe the system's solid components:

$$\rho C_{p,s} \frac{\delta T_s}{\delta t} = \nabla \cdot (k_s \nabla T_s) \quad (4)$$

### 2.6.3 Phase Change Material (PCM)

An enthalpy-porosity approach is utilised to model the melting process in PCM. Indeed, each cell in the solution region utilises a liquid fraction (the fraction of cell volume when it is in liquid form). In Ansys Fluent model selection, solidification and melting are chosen. The following mass and momentum equation used in enthalpy-porosity approach:

$$\frac{\delta \rho}{\delta t} + \nabla \cdot (\rho \cdot \vec{V}) = 0 \quad (5)$$

$$\rho \left[ \frac{\delta \vec{V}}{\delta t} + (\vec{V} \cdot \nabla) \vec{V} \right] = - \nabla P + \nabla \cdot (\mu \nabla \vec{V}) + S \quad (6)$$

$$S = \frac{(1-\beta)^2}{(\beta^3 + \phi)} A (\vec{V} - \vec{V}_p) \quad (7)$$

where  $\beta$  refers to liquid volume fraction, A refers to liquid fraction constant zone which equal to  $10^5$ ,  $\vec{V}_p$  refers to solid velocity due to the pulling velocity of solidified material out of the field,  $\phi$  refers to slight number to prevent zero division and equal to 0.001. As a result, the following is the energy equation:

$$\frac{\delta}{\delta t} (\rho H) + \nabla \cdot (\rho \vec{V} H) = \nabla \cdot (k \nabla T) + S \quad (8)$$

where  $H$ ,  $\rho$ ,  $\vec{V}$  and  $S$  are enthalpy of material, density, fluid velocity and source term, respectively. Combination of sensible and latent heat in enthalpy of material can be computed as:

$$H = h + \Delta H \quad (9)$$

where  $h$  and  $\Delta H$  are enthalpy of material of sensible enthalpy and latent enthalpy, respectively. Sensible enthalpy can be computed as:

$$h = h_{ref} + \int_{T_{ref}}^T C_p dT \quad (10)$$

where  $h_{ref}$  refers to enthalpy reference and  $T_{ref}$  refers to reference temperature. On the other side, the latent heat can be computed as:

$$\Delta H = \beta L \quad (11)$$

where  $L$  refers to latent heat. The latent heat of materials is various from solid (0) to liquid (L). The liquid fraction,  $\beta$  of latent heat are as follows:

$$\beta = \begin{cases} 0 & \text{if } T \leq T_{solidus} \\ \frac{T - T_{solidus}}{T_{liquidus} - T_{solidus}} & \text{if } T_{solidus} < T < T_{liquidus} \\ 1 & \text{else } T \geq T_{liquidus} \end{cases} \quad (12)$$

Heat absorption by PCM,  $E_{PCM}$  are defined as:

$$E_{PCM} = m_{PCM} \cdot C_{PCM} \cdot \Delta T \quad (13)$$

where  $m_{PCM}$ ,  $C_{PCM}$  and  $\Delta T$  are mass of PCM, specific heat capacity of PCM and temperature change of the working fluid.

#### 2.6.4 Thermodynamics analysis

In the performance of solar PVT-PCM, the analysis involved is thermodynamic analysis. There are two type of thermodynamics analysis which are energy analysis (first law of thermodynamic) and exergy analysis (second law of thermodynamics). In this research, the performance is evaluated using the energy analysis (first law of thermodynamic).

Energy from the sunlight is absorbed by the PV cells in the panel. Solar radiation in Ansys Fluent setup is liable to boundary condition. The incident solar radiation of the system,  $E_{sun}$  can be expressed as:

$$E_{sun} = \tau_g \cdot \alpha_{cell} \cdot A_{PV} \cdot G \quad (14)$$

where  $\tau_g$ ,  $\alpha_{cell}$ ,  $A_{PV}$  and  $G$  are transmissivity of the glass cover, absorptivity of the PV cells, solar PV panel area and rate of total solar irradiation, respectively. The energy relating to mass flow is calculated as:

$$E_{mass,out} - E_{mass,in} = E_{th} = m_f \cdot C_{p,f} \cdot (T_{f,out} - T_{f,in}) \quad (15)$$

where  $m_f$  refers to mass flow rate,  $C_{p,f}$  refers to specific heat capacity,  $T_{f,in}$  refers to temperature of inlet working fluid and  $T_{f,out}$  refers to temperature of outlet working fluid.

The thermal efficiency of the PVT system is expressed by:

$$\eta_{th} = \frac{E_{th}}{E_{sun}} = \frac{m_f \cdot C_{p,f} \cdot (T_{f,out} - T_{f,in})}{\tau_g \cdot \alpha_{cell} \cdot A_{PV} \cdot G} \quad (16)$$

Due to the present of PCM in the system, the thermal efficiency of the PVT-PCM system is calculated as:

$$\eta_{th} = \frac{m_f \cdot C_{p,f} \cdot (T_{f,out} - T_{f,in}) + E_{PCM}}{\tau_g \cdot \alpha_{cell} \cdot A_{PV} \cdot G} \quad (17)$$

where  $E_{PCM}$  is the thermal power absorbed by PCM. The thermal power absorbed by PCM is expressed as follow:

$$E_{PCM} = \begin{cases} \frac{m_{PCM} \cdot C_{P,PCM} \cdot (T_{PCM,t} - T_{PCM,t_0})}{t - t_0} & t < t_1 \\ \frac{m_{PCM} \cdot C_{P,PCM} \cdot (T_{PCM,t_1} - T_{PCM,t_0})}{t_1 - t_0} + \frac{m_{PCM} \cdot h}{t - t_1} & t_1 \leq t \leq t_2 \\ \frac{m_{PCM} \cdot C_{P,PCM} \cdot (T_{PCM,t_1} - T_{PCM,t_0})}{t_1 - t_0} + \frac{m_{PCM} \cdot h}{t_2 - t_1} + \frac{m_{PCM} \cdot C_{P,PCM} \cdot (T_{PCM,t} - T_{PCM, melting})}{t - t_2} & t > t_2 \end{cases} \quad (18)$$

The electrical efficiency of the system is expressed by:

$$\eta_{el} = \frac{E_{el}}{E_{sun}} = \eta_r \cdot [1 - 0.0045 \cdot (T_{cell} - 298.15)] \quad (19)$$

where  $\eta_r$  and  $T_{cell}$  refers to PV module efficiency at standard test condition and PV cells operating temperature.

Hence, overall efficiency of the system,  $\eta_{ov}$  are calculated as:

$$\eta_{ov} = \eta_{th} + \eta_{el} \quad (20)$$

### 3. Grid Independence Study and Model Validation

#### 3.1 Grid Independent Study

The precision of the simulation is improved by increasing the computational grid resolution, but the computational cost is also increased. Grid independence test is necessary to determine the ideal arrangement in terms of the number of computational cells. There are 3 grids utilized consists of coarse, medium, fine used in the grid independence study. The average difference in outlet temperature is between 0.01% – 0.03% which are relatively small. On the other hand, the average difference in surface temperature is 0.31% - 0.13%. Since both of the results produces small changes in the results, the simulation meshing type can be put a stop at medium meshing to reduce the computational cost and save more time as supported by Khanna *et al.*, [27].

#### 3.2 Model Validation

The validation studies have been investigated and compared from research by Kazemian *et al.*, [21] as a major reference for validation and compared with the present study. Kazemian *et al.*, [21] stated the inlet temperature of coolant flow of 30 °C, mass flow rate of the coolant flow is 30 kg/h, ambient temperature of 30 °C, solar radiation of 800 W/m<sup>2</sup> and wind speed of 1 m/s. In addition, the thermophysical properties of the Phase Change Material (PCM) such as melting point of the PCM is 55 °C is chosen similar to Kazemian *et al.*, [21]. Furthermore, further thermophysical properties of

PCM such as density equals to  $800 \text{ kg/m}^3$ , enthalpy of fusion equals to  $170 \text{ kJ/kg}$ , the thermal conductivity is  $0.25 \text{ W/m.K}$  and heat capacity is  $2300 \text{ J/kg.K}$ .

The results of the PVT-PCM are investigated on several parts such as surface and outlet temperature to study on the performance. The uppermost layer of the PVT-PCM is considered as surface layer. At the final step in the simulation, the highest temperature produced at the surface of the present study are  $57.39 \text{ }^\circ\text{C}$  while the Kazemian *et al.*, [21] shows  $55.54 \text{ }^\circ\text{C}$ . The average percentage difference of surface temperature between present study and the study by Kazemian *et al.*, [21] shows  $4.70\%$ . The value of the coefficient of determination (R-squared) is  $2.40$  corresponds to high reliability of this research.

At the end of the simulation, the greatest temperature created at the outlet temperature of the present study is  $33.34 \text{ }^\circ\text{C}$ , while the highest temperature produced by Kazemian *et al.*, [21] study is  $33 \text{ }^\circ\text{C}$ . The average percentage difference of outlet temperature between the both studies show  $0.66\%$ . The value of the coefficient of determination (R-squared) is  $0.52$  indicates reasonable accuracy and reliability of this research.

#### 4. Results and Discussion

In this present study, the simulation model of PVT-PCM is developed under constant solar irradiance which is  $450 \text{ W/m}^2$ . The initial temperature of the working fluid started with  $30 \text{ }^\circ\text{C}$ . The selected PCM used is RT44HC as the thermophysical properties are presented in Table 3. Parametric analyses are developed to determine the influence of various parameters on the performance of the PVT-PCM. Parameters included in this study are variation of mass flow rate, various solar irradiance on PVT-PCM system will be investigated and the comparative analysis between PVT and PVT-PCM.

##### 4.1 Performance of PVT-PCM on Various Mass Flow Rate at Constant Solar Irradiance

In this parametric analysis, the effect of various mass flow rate on the surface and outlet temperature are exhibited in this section. Four different mass flow rate of  $10 \text{ kg/h}$ ,  $30 \text{ kg/h}$ ,  $50 \text{ kg/h}$  and  $70 \text{ kg/h}$  are selected for these numerical analyses.

Figure 3 shows the surface temperature of the PVT-PCM on various mass flow rate. Despite the results of the surface temperature under mass flow rate  $10 \text{ kg/h}$  operation shows the highest temperature. On the other hand, mass flow rate of  $70 \text{ kg/h}$  shows the lowest temperature while other mass flow rate differences are not significant.

The results of variation of outlet temperature by applying using various mass flow rate are shown in Figure 4. The mass flow rate of  $10 \text{ kg/h}$  shows the significant temperature at the outlet as compared to  $30 \text{ kg/h}$ ,  $50 \text{ kg/h}$  and  $70 \text{ kg/h}$ . As the mass flow rate increases from  $10 \text{ kg/h}$  to  $70 \text{ kg/h}$ , the average outlet temperature of the PVT-PCM decreases from  $41.32 \text{ }^\circ\text{C}$  to  $31.93 \text{ }^\circ\text{C}$ . Additionally, increasing in the mass flow rate reduces the temperature of the outlet since the system requires higher outlet temperature to increase the electrical efficiency of the PVT-PCM. However, higher mass flow rate will reduce the thermal efficiencies.

Increasing in mass flow rate leads in a higher Reynolds number. Subsequently, the flow turbulence and heat transfer coefficient will be escalated. It could be argued that the increased in flow rate requires stronger pumps which increase the total cost of the system. Therefore, identifying the optimal flow rate might help to achieve an appropriate thermal efficiency while sustain in low costs.

Referring to Table 6 are the performance of PVT-PCM on variation of mass flow rate. Based on the simulation output, by increasing the mass flow rate of the working fluid from  $10 \text{ kg/h}$  to  $70 \text{ kg/h}$ ,

the thermal efficiencies decrease while the electrical efficiencies increase. By increasing of mass flow rate from 10 kg/h to 70 kg/h, the thermal efficiency of PVT-PCM system decreases from 73.08% to 72.18% and electrical efficiency increases from 17.74% to 18.27%. Therefore, the overall efficiencies decrease as the mass flow rate increases from 10kg/h to 70 kg/h by 90.82% to 90.46%, respectively. As a consequence of the reduction in average surface and outlet temperature by increasing the mass flow rate of the working fluid.

**Table 6**  
 Performance of PVT-PCM on Various Mass Flow Rate

Mass Flow Rate (kg/h)	Thermal Efficiency (%)	Electrical Efficiency (%)	Overall Efficiency (%)
10	73.08	17.74	90.82
30	72.43	18.11	90.54
50	72.26	18.22	90.48
70	72.18	18.27	90.46

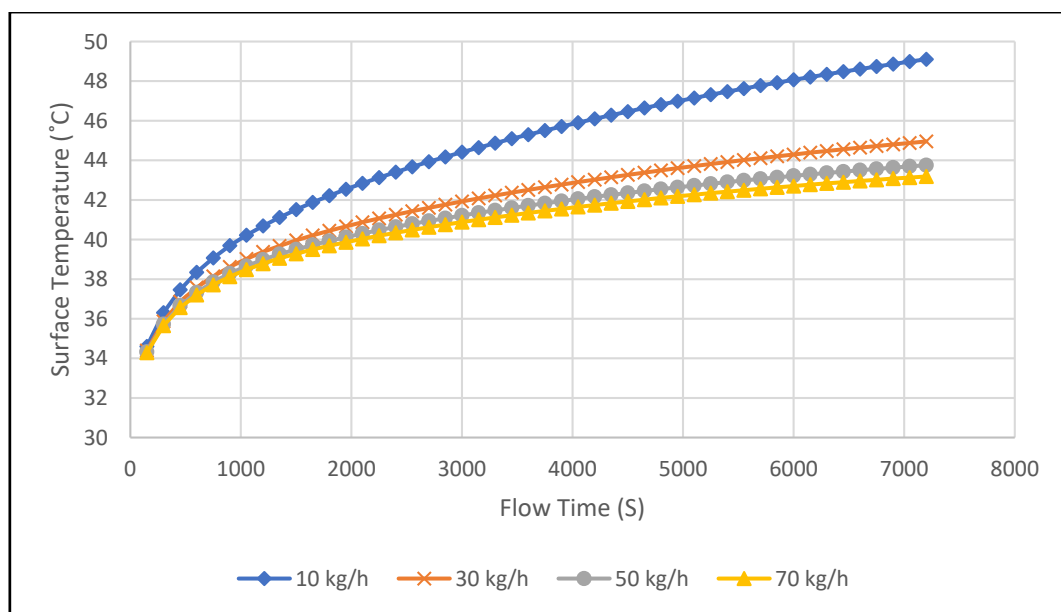


**Fig. 3.** Surface Temperature of PVT-PCM on Various Mass Flow Rate at Constant Solar Irradiance 450 W/m<sup>2</sup>

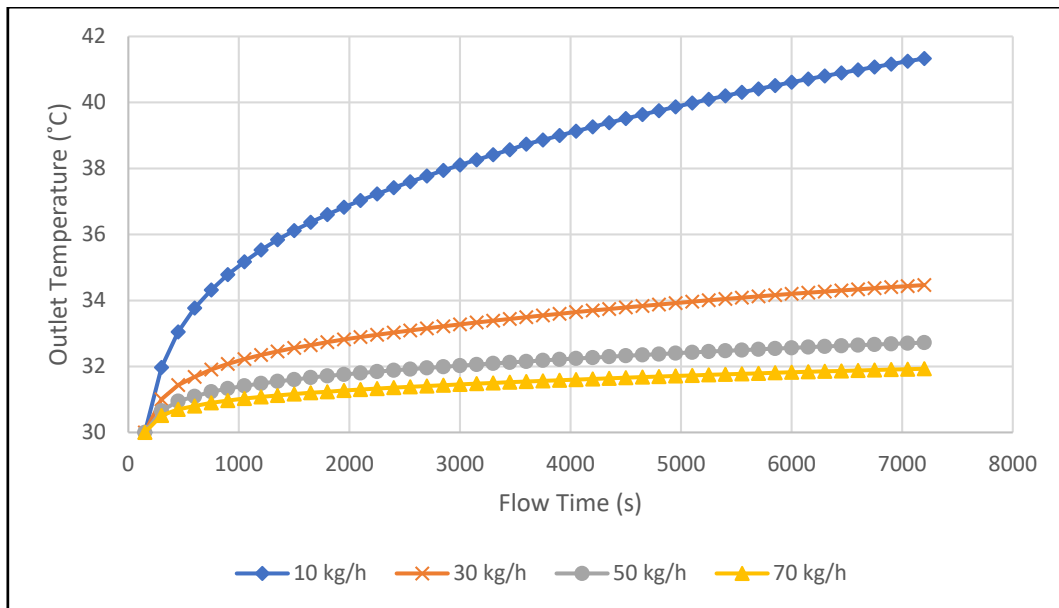


**Fig. 4.** Outlet Temperature of PVT-PCM on Various Mass Flow Rate at Constant Solar Irradiance  $450 \text{ W/m}^2$

#### 4.2 Performance of PVT-PCM on Various Mass Solar Irradiance at Constant Mass Flow Rate

In this section, the outlet temperature on various solar irradiance at constant mass flow rate of  $10 \text{ kg/h}$  as shown in Figure 5. The variation of solar irradiance starts from the lowest irradiance until the highest irradiance. The lowest irradiance indicated by  $200 \text{ W/m}^2$ , middle irradiance by  $450 \text{ W/m}^2$  and the highest irradiance by  $800 \text{ W/m}^2$ . The highest temperature of the outlet shows  $50.13^\circ\text{C}$  by  $800 \text{ W/m}^2$  irradiance. Referring to the Figure 5, the outlet temperature increases as the solar irradiance increases. In this study the solar irradiance used was  $450 \text{ W/m}^2$  shows results by  $41.32^\circ\text{C}$  while the lowest irradiance of  $200 \text{ W/m}^2$  shows with  $35.03^\circ\text{C}$ . The percentage difference between  $800 \text{ W/m}^2$  and  $450 \text{ W/m}^2$  was 19.26%. On the other hand, the difference between  $450 \text{ W/m}^2$  and  $200 \text{ W/m}^2$  are 16.48%, both differences show almost similar difference. This shows a uniform change in the outlet temperature proportional to the flow time.

Thus, this shows the increment of solar irradiance will be affected with the increasing of outlet temperature. The solar irradiance will be absorbed by the EVA panel of the system and transferred into the PCM layer. Next, the heat absorbed by the PCM and being transferred to the copper tube collector which contains the working fluid.

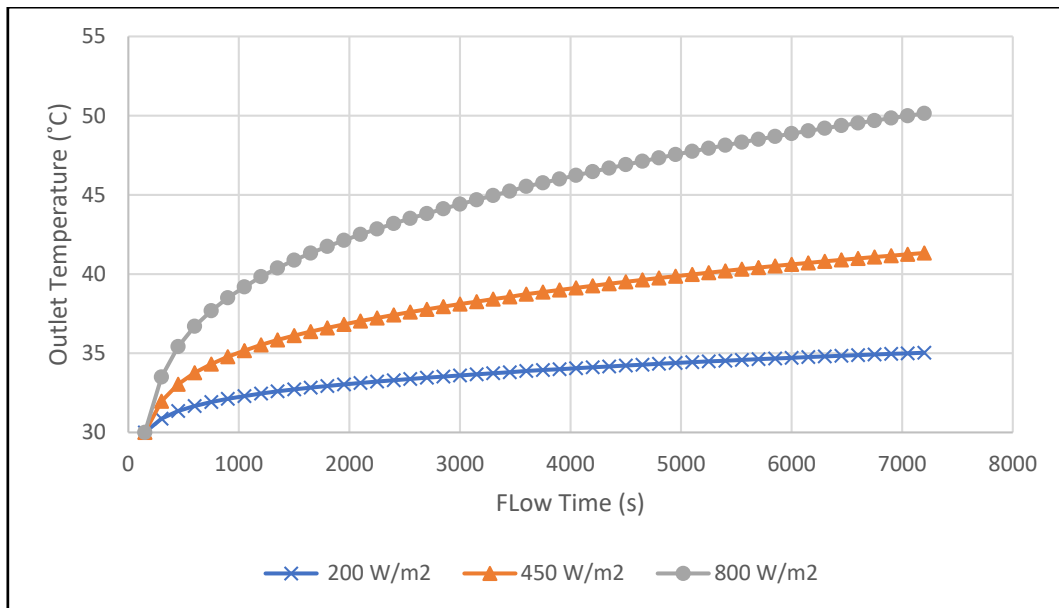


**Fig. 5.** Outlet Temperature on Various Solar Irradiance at Constant Mass Flow Rate 10kg/h

Referring to the Figure 6, the results of surface temperature on the variation of solar irradiance at constant mass flow rate of 10 kg/h. Based on the simulation, by increasing the solar irradiance from 200 W/m<sup>2</sup> to 800 W/m<sup>2</sup>, the average surface temperatures increase from 38.49°C to 63.96°C. At the medium level of 450 W/m<sup>2</sup> solar irradiance, the surface temperature shows 49.10°C. The percentage difference between low-medium and medium-high irradiance are 24.23% and 26.28%, respectively. At initial flow time 150s, the temperature started to rises slowly because PCM still in solid state. It can be seen that the temperature rises as the flow time pass until 7200s and the PCM encounter melting process.

Performance of thermal efficiency and electrical efficiency by the variation of solar irradiance as illustrated in Table 7. By increasing of solar irradiance from 200 W/m<sup>2</sup> to 800 W/m<sup>2</sup>, the thermal efficiency of PVT-PCM system increases from 72.48 % to 73.91%. On the other hand, the electrical efficiency decreases from 18.69% to 16.41%. Furthermore, the average percentage difference between the highest and lowest irradiance at thermal efficiency and electrical efficiency are 1.96% and 12.99%, respectively. Therefore, Table 7 shows the results of overall efficiencies by 200 W/m<sup>2</sup>, 450 W/m<sup>2</sup> and 800 W/m<sup>2</sup> are 91.17%, 90.82% and 90.33%, respectively. As the solar irradiance increases, the thermal efficiency of the PVT-PCM increases due to heat transfer occurrence in the PVT-PCM. However, it can be seen that by increasing the solar irradiance, the overall performance will drop accordingly. As results, heat can severely reduce the power production in solar PVT.

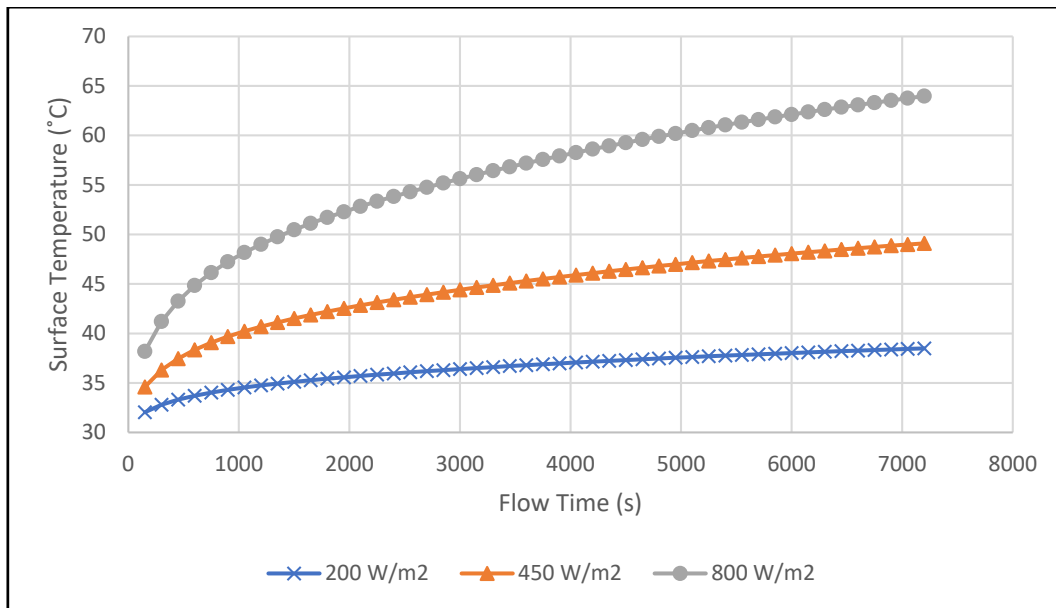
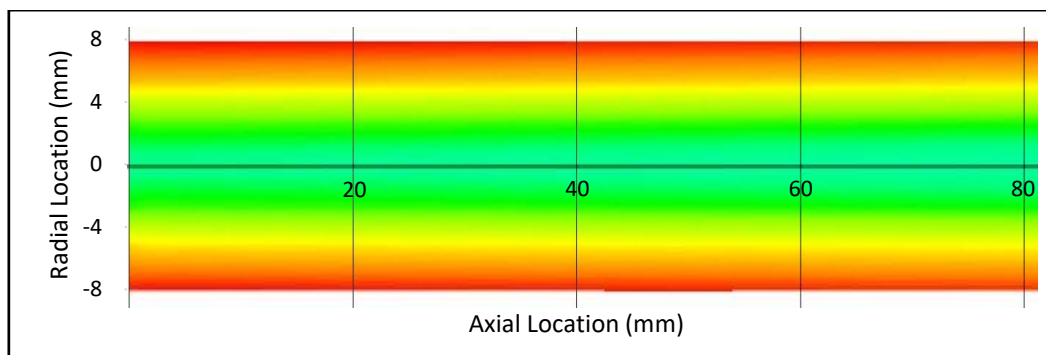


**Fig. 6.** Surface Temperature on Various Solar Irradiance at Constant Mass Flow Rate 10kg/h

**Table 7**  
 Performance of PVT-PCM on Various Solar Irradiance

Irradiance (W/m <sup>2</sup> )	Thermal Efficiency (%)	Electrical Efficiency (%)	Overall Efficiency (%)
200	72.48	18.69	91.17
450	73.08	17.74	90.82
800	73.92	16.41	90.33

The axial flow assembles from the inlet to the outlet of the working fluid in the copper tube. The axial temperature examined from the outlet point denoted as 0mm through 80mm inwards. Figure 7 shows the axial temperature distribution at the outlet of the working fluid and axial temperature profile for 200 W/m<sup>2</sup>, 450 W/m<sup>2</sup>, 800 W/m<sup>2</sup>.



(a)

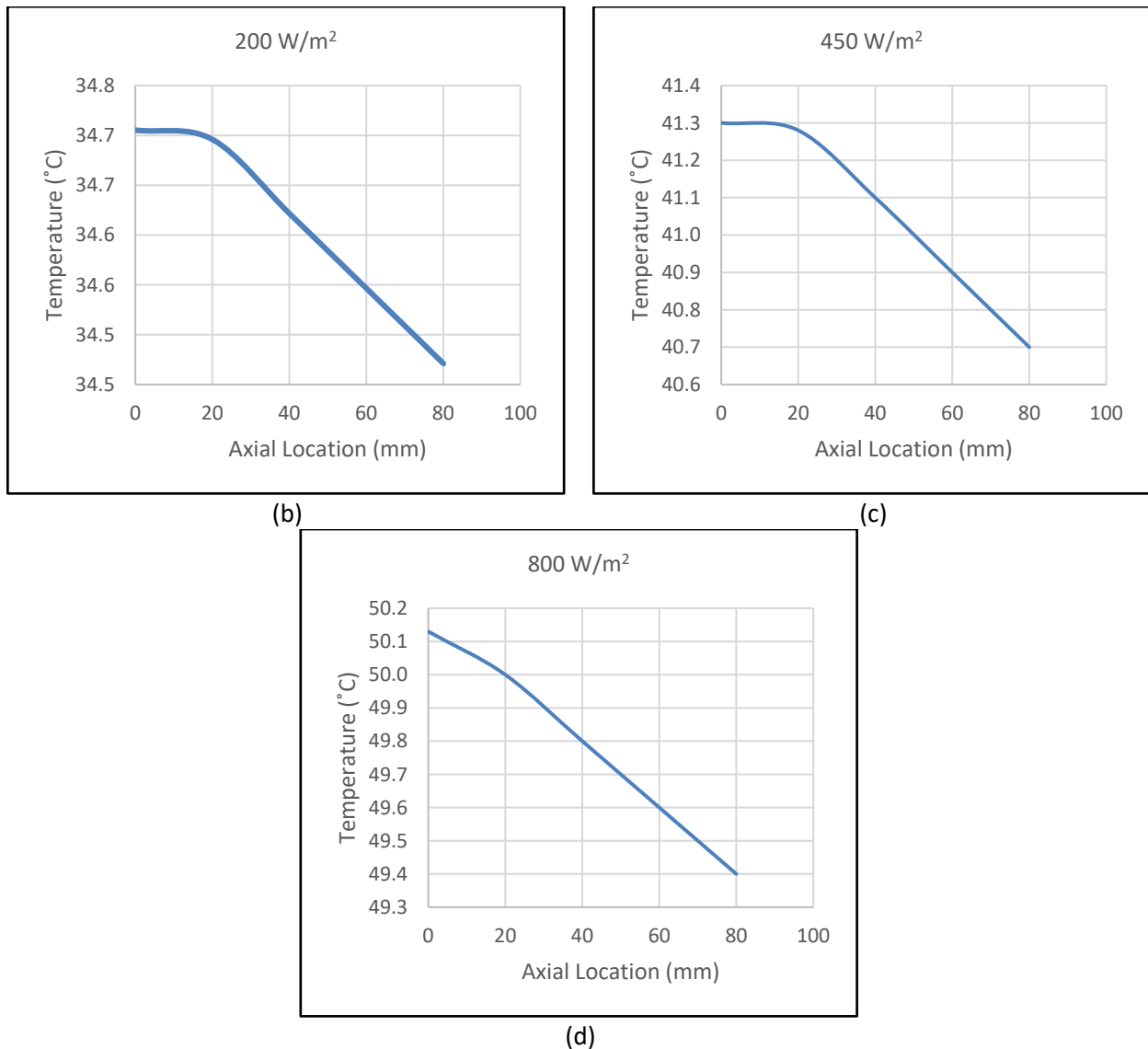


**Fig. 7.** (a) Axial Temperature Distribution (b) Axial Temperature Profile at 200 W/m<sup>2</sup> (c) Axial Temperature Profile at 450 W/m<sup>2</sup> (d) Axial Temperature Profile at 800 W/m<sup>2</sup>

#### 4.3 Comparison Between PVT and PVT-PCM

In the comparison of PVT and PVT-PCM, the geometry by PVT is designed with the absence of Phase Change Material (PCM). The surface and outlet temperature of the PVT-PCM are examined using the similar boundary condition and operating condition. Both systems undergo 7200s simulation transiently, at constant solar irradiance of 450 W/m<sup>2</sup>, mass flow rate of coolant flow at 10 kg/h and initial temperature of coolant flow at 30°C.

Figure 8 compares the temperature at the outlet between PVT and PVT-PCM. The outlet temperature from the PVT system rises rapidly at initial stage and started to be constant at 2000s. The final temperature of the outlet by PVT and PVT-PCM shows 44.76°C and 41.32°C, respectively. The outlet temperature of the PVT is 7.98% higher than PVT-PCM system. These findings provide additional evidence when the outlet temperature from the PVT-PCM system is lower than PVT system due heat absorption by the PCM and the excessive heat is reduced when transferred to the working fluid. Khodadadi and Sheikholeslami [35] support the idea of the outlet temperature of the PVT-PCM system are lower than PVT system.

Figure 9 provides the surface temperature between PVT and PVT-PCM. The final simulation output of surface temperature by PVT and PVT-PCM exhibits 54.12°C and 49.10°C, respectively. The percentage difference of PVT system is 9.72% higher than PVT-PCM system. Interestingly, this correlation is related to the temperature of PVT and the performance of both systems. These are remarkable results since lower temperature of surface temperature will produce higher efficiency of the PVT-PCM system. This study has been demonstrated by Navazani *et al.*, [36] and Abdullah *et al.*, [37] stated that the lower temperature, the higher the efficiency of the system.

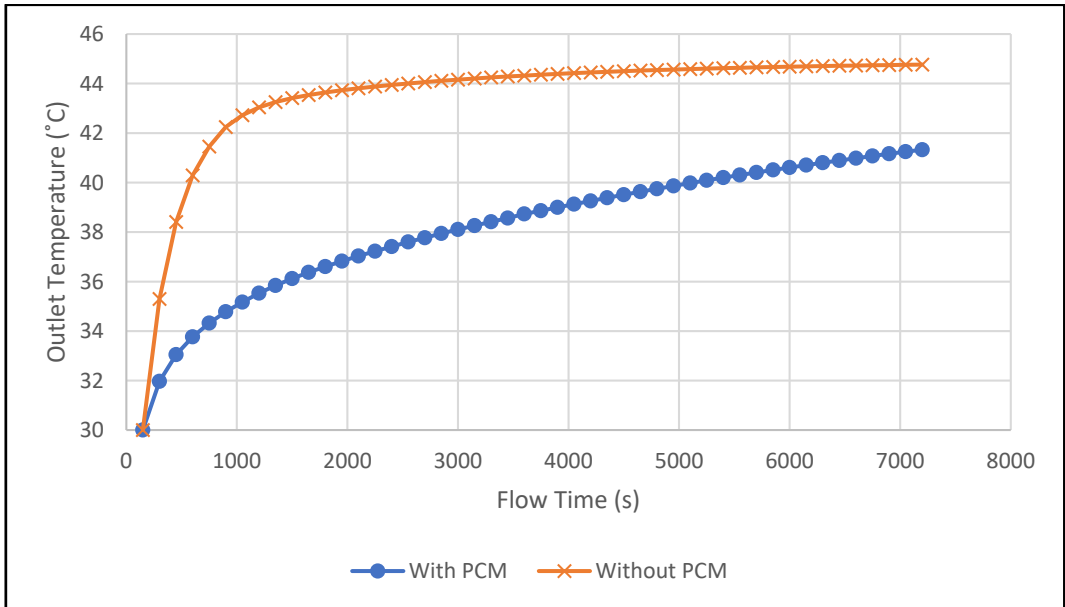


Fig. 8. Comparison of Outlet Temperature between PVT and PVT-PCM

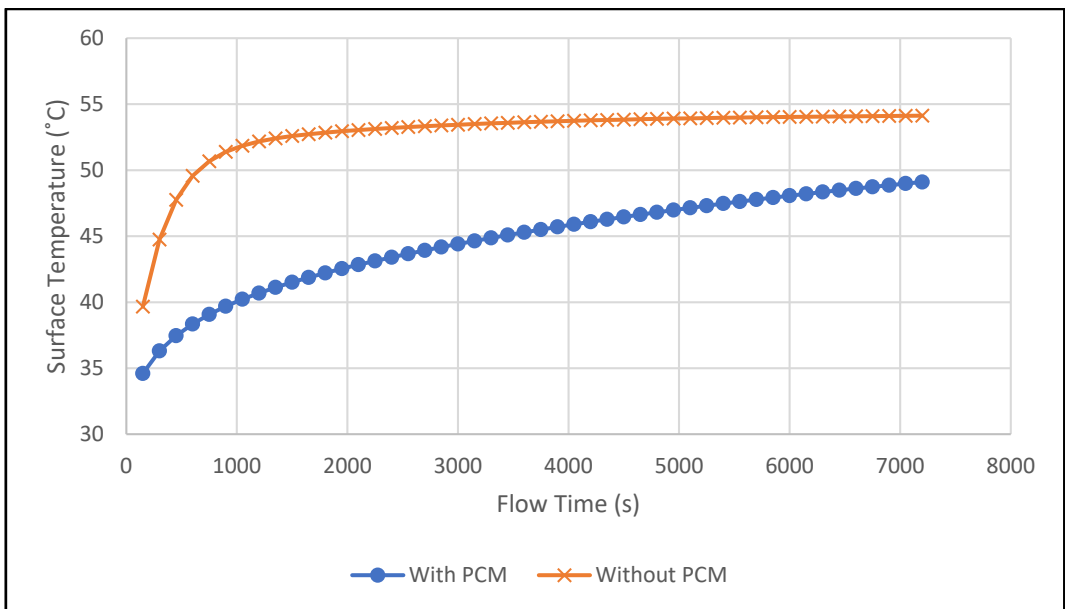


Fig. 9. Comparison of Surface Temperature between PVT and PVT-PCM

## 5. Conclusion

Finally, this paper presented numerical investigation of PCM acts as promising elements incorporated in the PVT system that have the capability to reduce the temperature of the PVT-PCM system. The optimum parameters in the thermal efficiencies when the mass flow rate is lower to allowed better heat transfer process from the surface to the PCM [38]. In contrast, reduction in the mass flow rate, the electrical efficiencies will be reduced.

Solar irradiances are other parameters considered in this study. The increasing of solar irradiance leads to thermal efficiency growth. Alternately, higher solar irradiance leads to reduction in electrical efficiencies due to the undesirable temperature of the PVT-PCM system and reduce the power production [39-41]. In accordance with the variation of parameters supplementary will influence of the performance of PVT-PCM [42]. Conclusively, Phase Change Materials (PCMs) are a potential technology for thermal energy storage to store and release a considerable quantity of latent [43].

## Acknowledgement

The author appreciates the facilities and equipment provided by the Faculty of Mechanical Engineering, Applied Solar Energy Laboratory (ASEL) and Universiti Teknikal Malaysia Melaka (UTeM) to support this research. This research was not funded by any grant.

## References

- [1] Chandrasekar, M., and T. Senthilkumar. "Five decades of evolution of solar photovoltaic thermal (PVT) technology- A critical insight on review articles." *Journal of Cleaner Production* 322 (2021): 128997. <https://doi.org/10.1016/j.jclepro.2021.128997>
- [2] Hu, Guangtao, Xing Ning, Muzamil Hussain, Uzair Sajjad, Muhammad Sultan, Hafiz Muhammad Ali, Tayyab Raza Shah, and Hassaan Ahmad. "Potential evaluation of hybrid nanofluids for solar thermal energy harvesting: A review of recent advances." *Sustainable Energy Technologies and Assessments* 48 (2021): 101651. <https://doi.org/10.1016/j.seta.2021.101651>
- [3] Shah, Tayyab Raza, and Hafiz Muhammad Ali. "Applications of hybrid nanofluids in solar energy, practical limitations and challenges: a critical review." *Solar Energy* 183 (2019): 173-203. <https://doi.org/10.1016/j.solener.2019.03.012>
- [4] Rebhi, Redha, Younes Menni, Giulio Lorenzini, and Hijaz Ahmad. "Forced-Convection Heat Transfer in Solar Collectors and Heat Exchangers: A Review." *Journal of Advanced Research in Applied Sciences and Engineering Technology* 26, no. 3 (2022): 1-15. <https://doi.org/10.37934/araset.26.3.115>
- [5] Sachit, F. A., M. A. M. Rosli, N. Tamaldin, S. Misha, and A. L. Abdullah. "Nanofluids used in photovoltaic thermal (pv/t) systems." *International Journal of Engineering & Technology* 7, no. 3.20 (2018): 599-611.
- [6] Abdul-Ganiyu, Saeed, David A. Quansah, Emmanuel W. Ramde, Razak Seidu, and Muyiwa S. Adaramola. "Study effect of flow rate on flat-plate water-based photovoltaic-thermal (PVT) system performance by analytical technique." *Journal of Cleaner Production* 321 (2021): 128985. <https://doi.org/10.1016/j.jclepro.2021.128985>
- [7] Fu, Zaiguo, Yongwei Li, Xiaotian Liang, Shang Lou, Zhongzhu Qiu, Zhiyuan Cheng, and Qunzhi Zhu. "Experimental investigation on the enhanced performance of a solar PVT system using micro-encapsulated PCMs." *Energy* 228 (2021): 120509. <https://doi.org/10.1016/j.energy.2021.120509>
- [8] Qiu, Lin, Yuxin Ouyang, Yanhui Feng, and Xinxin Zhang. "Review on micro/nano phase change materials for solar thermal applications." *Renewable Energy* 140 (2019): 513-538. <https://doi.org/10.1016/j.renene.2019.03.088>
- [9] Thakur, Abhishek, Raj Kumar, Sushil Kumar, and Pawan Kumar. "Review of developments on flat plate solar collectors for heat transfer enhancements using phase change materials and reflectors." *Materials Today: Proceedings* 45 (2021): 5449-5455. <https://doi.org/10.1016/j.matpr.2021.02.120>
- [10] Badieli, Z., M. Eslami, and K. Jafarpur. "Performance improvements in solar flat plate collectors by integrating with phase change materials and fins: A CFD modeling." *Energy* 192 (2020): 116719. <https://doi.org/10.1016/j.energy.2019.116719>
- [11] Lin, Saw Chun, Hussain H. Al-Kayiem, and M. S. Aris. "Experimental investigation on the performance enhancement of integrated PCM-flat plate solar collector." *Journal of Applied Sciences* 12, no. 23 (2012): 2390-2396. <https://doi.org/10.3923/jas.2012.2390.2396>

- [12] Preet, Sajan, Brij Bhushan, and Tarun Mahajan. "Experimental investigation of water based photovoltaic/thermal (PV/T) system with and without phase change material (PCM)." *Solar Energy* 155 (2017): 1104-1120. <https://doi.org/10.1016/j.solener.2017.07.040>
- [13] Khan, Mohammed Mumtaz A., Nasiru I. Ibrahim, I. M. Mahbulul, Hafiz Muhammad Ali, R. Saidur, and Fahad A. Al-Sulaiman. "Evaluation of solar collector designs with integrated latent heat thermal energy storage: a review." *Solar Energy* 166 (2018): 334-350. <https://doi.org/10.1016/j.solener.2018.03.014>
- [14] Abdullah, A. S., Z. M. Omara, F. A. Essa, M. M. Younes, S. Shanmugan, Mohamed Abdelgaied, M. I. Amro, A. E. Kabeel, and W. M. Farouk. "Improving the performance of trays solar still using wick corrugated absorber, nano-enhanced phase change material and photovoltaics-powered heaters." *Journal of Energy Storage* 40 (2021): 102782. <https://doi.org/10.1016/j.est.2021.102782>
- [15] Mousavi, Soroush, Alibakhsh Kasaeian, Mohammad Behshad Shafii, and Mohammad Hossein Jahangir. "Numerical investigation of the effects of a copper foam filled with phase change materials in a water-cooled photovoltaic/thermal system." *Energy Conversion and Management* 163 (2018): 187-195. <https://doi.org/10.1016/j.enconman.2018.02.039>
- [16] Wahab, Abdul, Muhammad Alam Zaib Khan, and Ali Hassan. "Impact of graphene nanofluid and phase change material on hybrid photovoltaic thermal system: Exergy analysis." *Journal of Cleaner Production* 277 (2020): 123370. <https://doi.org/10.1016/j.jclepro.2020.123370>
- [17] Hassan, Ali, Abdul Wahab, Muhammad Arslan Qasim, Muhammad Mansoor Janjua, Muhammad Aon Ali, Hafiz Muhammad Ali, Tufail Rehman Jadoon, Ejaz Ali, Ahsan Raza, and Noshairwan Javaid. "Thermal management and uniform temperature regulation of photovoltaic modules using hybrid phase change materials-nanofluids system." *Renewable Energy* 145 (2020): 282-293. <https://doi.org/10.1016/j.renene.2019.05.130>
- [18] Shalaby, S. M., E. El-Bialy, and A. A. El-Sebaei. "An experimental investigation of a v-corrugated absorber single-basin solar still using PCM." *Desalination* 398 (2016): 247-255. <https://doi.org/10.1016/j.desal.2016.07.042>
- [19] Al-Musawi, Ahmed Issa Abbood, Amin Taheri, Amin Farzanehnia, Mohammad Sardarabadi, and Mohammad Passandideh-Fard. "Numerical study of the effects of nanofluids and phase-change materials in photovoltaic thermal (PVT) systems." *Journal of Thermal Analysis and Calorimetry* 137, no. 2 (2019): 623-636. <https://doi.org/10.1007/s10973-018-7972-6>
- [20] Al-Waeli, Ali HA, Miqdam T. Chaichan, Kamaruzzaman Sopian, Hussein A. Kazem, Hameed B. Mahood, and Anees A. Khadom. "Modeling and experimental validation of a PVT system using nanofluid coolant and nano-PCM." *Solar Energy* 177 (2019): 178-191. <https://doi.org/10.1016/j.solener.2018.11.016>
- [21] Kazemian, Arash, Ali Salari, Ali Hakkaki-Fard, and Tao Ma. "Numerical investigation and parametric analysis of a photovoltaic thermal system integrated with phase change material." *Applied Energy* 238 (2019): 734-746. <https://doi.org/10.1016/j.apenergy.2019.01.103>
- [22] Naghdbishi, Ali, Mohammad Eftekhari Yazdi, and Ghasem Akbari. "Experimental investigation of the effect of multi-wall carbon nanotube-Water/glycol based nanofluids on a PVT system integrated with PCM-covered collector." *Applied Thermal Engineering* 178 (2020): 115556. <https://doi.org/10.1016/j.applthermaleng.2020.115556>
- [23] Salari, Ali, Arash Kazemian, Tao Ma, Ali Hakkaki-Fard, and Jinqing Peng. "Nanofluid based photovoltaic thermal systems integrated with phase change materials: Numerical simulation and thermodynamic analysis." *Energy Conversion and Management* 205 (2020): 112384. <https://doi.org/10.1016/j.enconman.2019.112384>
- [24] Sopian, Kamaruzzaman, Ali HA Al-Waeli, and Hussein A. Kazem. "Energy, exergy and efficiency of four photovoltaic thermal collectors with different energy storage material." *Journal of Energy Storage* 29 (2020): 101245. <https://doi.org/10.1016/j.est.2020.101245>
- [25] Carmona, Mauricio, Alberto Palacio Bastos, and José Doria García. "Experimental evaluation of a hybrid photovoltaic and thermal solar energy collector with integrated phase change material (PVT-PCM) in comparison with a traditional photovoltaic (PV) module." *Renewable Energy* 172 (2021): 680-696. <https://doi.org/10.1016/j.renene.2021.03.022>
- [26] Khanjari, Y., A. B. Kasaeian, and F. Pourfayaz. "Evaluating the environmental parameters affecting the performance of photovoltaic thermal system using nanofluid." *Applied Thermal Engineering* 115 (2017): 178-187. <https://doi.org/10.1016/j.applthermaleng.2016.12.104>
- [27] Khanna, Sourav, K. S. Reddy, and Tapas K. Mallick. "Performance analysis of tilted photovoltaic system integrated with phase change material under varying operating conditions." *Energy* 133 (2017): 887-899. <https://doi.org/10.1016/j.energy.2017.05.150>
- [28] Hosseinzadeh, Mohammad, Ali Salari, Mohammad Sardarabadi, and Mohammad Passandideh-Fard. "Optimization and parametric analysis of a nanofluid based photovoltaic thermal system: 3D numerical model with experimental validation." *Energy Conversion and Management* 160 (2018): 93-108. <https://doi.org/10.1016/j.enconman.2018.01.006>

- [29] Malaysian Meteorological Department. "Monthly Weather Bulletin October 2021". *Kementerian Alam Sekitar dan Air*. Accessed 2021. <https://www.met.gov.my/data/climate/buletincuacabulanan.pdf>.
- [30] Shavalipour, Aghil, Mir Hamed Hakemzadeh, K. Sopian, Sallehuddin Mohamed Haris, and Saleem H. Zaidi. "New formulation for the estimation of monthly average daily solar irradiation for the tropics: a case study of Peninsular Malaysia." *International Journal of Photoenergy* 2013 (2013). <https://doi.org/10.1155/2013/174671>
- [31] Hossain, M. S., A. K. Pandey, Jeyraj Selvaraj, Nasrudin Abd Rahim, M. M. Islam, and V. V. Tyagi. "Two side serpentine flow based photovoltaic-thermal-phase change materials (PVT-PCM) system: Energy, exergy and economic analysis." *Renewable Energy* 136 (2019): 1320-1336. <https://doi.org/10.1016/j.renene.2018.10.097>
- [32] Su, Di, Yuting Jia, Yaxue Lin, and Guiyin Fang. "Maximizing the energy output of a photovoltaic-thermal solar collector incorporating phase change materials." *Energy and Buildings* 153 (2017): 382-391. <https://doi.org/10.1016/j.enbuild.2017.08.027>
- [33] Emam, Mohamed, and Mahmoud Ahmed. "Cooling concentrator photovoltaic systems using various configurations of phase-change material heat sinks." *Energy Conversion and Management* 158 (2018): 298-314. <https://doi.org/10.1016/j.enconman.2017.12.077>
- [34] Joshi, Anand S., and Arvind Tiwari. "Energy and exergy efficiencies of a hybrid photovoltaic-thermal (PV/T) air collector." *Renewable Energy* 32, no. 13 (2007): 2223-2241. <https://doi.org/10.1016/j.renene.2006.11.013>
- [35] Khodadadi, Mohammadjavad, and M. Sheikholeslami. "Numerical simulation on the efficiency of PVT system integrated with PCM under the influence of using fins." *Solar Energy Materials and Solar Cells* 233 (2021): 111402. <https://doi.org/10.1016/j.solmat.2021.111402>
- [36] Navazani, Shiva, Narges Yaghoobi Nia, Mahmoud Zendehtdel, Ali Shokuhfar, and Aldo Di Carlo. "Fabrication of high efficiency, low-temperature planar perovskite solar cells via scalable double-step crystal engineering deposition method fully out of glove box." *Solar Energy* 206 (2020): 181-187. <https://doi.org/10.1016/j.solener.2020.05.084>
- [37] Abdullah, Amira Lateef, Suhaimi Misha, Noreffendy Tamaldin, Mohd Afzanizam Mohd Rosli, and Fadhil Abdulameer Sachit. "Hybrid photovoltaic thermal PVT solar systems simulation via Simulink/Matlab." *CFD Letters* 11, no. 4 (2019): 64-78.
- [38] Azimi, Neda, Yegane Davoodbeygi, Masoud Rahimi, Shahin Ahmadi, Ehsan Karami, and Mahdi Roshani. "Optimization of thermal and electrical efficiencies of a photovoltaic module using combined PCMs with a thermo-conductive filler." *Solar Energy* 231 (2022): 283-296. <https://doi.org/10.1016/j.solener.2021.11.066>
- [39] Sukri, M. F., M. A. Salim, MA Mohd Rosli, S. B. Azraai, and R. Mat Dan. "An analytical investigation of overall thermal transfer value on commercial building in Malaysia." *International Review of Mechanical Engineering* 6, no. 5 (2012): 1050-1056.
- [40] Revichandran, Rajeenderan, Jaffar Syed Mohamed Ali, Moumen Idres, and A. K. M. Mohiuddin. "Energy Efficiency and Optimization of Buildings for Sustainable Development in Malaysia." *Journal of Advanced Research in Fluid Mechanics and Thermal Sciences* 93, no. 2 (2022): 28-36. <https://doi.org/10.37934/arfmts.93.2.2836>
- [41] Rosli, Mohd Afzanizam Mohd, Muhammad Zaid Nawam, Irfan Alias Farhan Latif, Safarudin Ghazali Herawan, Noriffah Md Noh, Siti Nur Dini Noordin Saleem, and Faridah Hussain. "The Effect of Variation in Mass Flow Rate and Solar Irradiance on Temperature Uniformity and Thermal Performance of Photovoltaic Thermal: A Simulated CFD Study." *Journal of Advanced Research in Fluid Mechanics and Thermal Sciences* 91, no. 2 (2022): 106-119. <https://doi.org/10.37934/arfmts.91.2.106119>
- [42] Sachit, F. A., Noreffendy Tamaldin, M. A. M. Rosli, S. Misha, and A. L. Abdullah. "Current progress on flat-plate water collector design in photovoltaic thermal (PV/T) systems: A Review." *Journal of Advanced Research in Dynamical and Control Systems* 10, no. 4 (2018): 680-89.
- [43] Mohd Rosli, Mohd Afzanizam, Sohif Mat, Kamaruzzaman Sopian, Mohd Yusof Sulaiman, Elias Ilias Salleh, and Mohd Khairul Anuar Sharif. "Thermal performance on unglazed photovoltaic thermal polymer collector." In *Advanced Materials Research*, vol. 911, pp. 238-242. Trans Tech Publications Ltd, 2014. <https://doi.org/10.4028/www.scientific.net/AMR.911.238>